Обверткин И.В., Пасечник К.А., Власов А.Ю. Потенциал использования одностенных и многостенных углеродных нанотрубок и углеродных нановолокон в качестве модификаторов полимерной матрицы, способных увеличить размеростабильность и технологическую устойчивость композиционного материала // Вестник Пермского национального исследовательского политехнического университета. Механика. – 2021. – № 4. – С. 98–110. DOI: 10.15593/perm.mech/2021.4.10

Obvertkin I.V., Pasechnik K.A., Vlasov A.Y. The potential of using SWCNTs, MWCNTs and CNFs capable of increasing the composite material dimensional and technological stability as modifiers of a polymer matrix. *PNRPU Mechanics Bulletin*, 2021, no. 4, pp. 98-110. DOI: 10.15593/perm.mech/2021.4.10

ВЕСТНИК ПНИПУ. МЕХАНИКА
№ 4, 2021
PNRPU MECHANICS BULLETIN
https://ered.pstu.ru/index.php/mechanics/index

DOI: 10.15593/perm.mech/2021.4.10
УДК 620.1/.2

ПОТЕНЦИАЛ ИСПОЛЬЗОВАНИЯ ОДНОСТЕННЫХ И МНОГОСТЕННЫХ УГЛЕРОДНЫХ НАНОТРУБОК И УГЛЕРОДНЫХ НАНОВОЛОКОН В КАЧЕСТВЕ МОДИФИКАТОРОВ ПОЛИМЕРНОЙ МАТРИЦЫ, СПОСОБНЫХ УВЕЛИЧИТЬ РАЗМЕРОСТАБИЛЬНОСТЬ И ТЕХНОЛОГИЧЕСКУЮ УСТОЙЧИВОСТЬ КОМПОЗИЦИОННОГО МАТЕРИАЛА

И.В. Обверткин, К.А. Пасечник, А.Ю. Власов

Сибирский государственный университет науки и технологий им. академика М.Ф. Решетнева, Красноярск, Россия

О СТАТЬЕ

Получена: 4 мая 2021 г.
Принята: 10 декабря 2021 г.
Опубликована: 30 декабря 2021 г.

Ключевые слова:

нанокомпозиты, углеродные нанотрубки и нановолокна, термомеханические характеристики, аналитическое моделирование, термический анализ.

АННОТАЦИЯ

В данной работе изучается влияние углеродных наночастиц, таких как углеродные нановолокна (УНВ), одностенные углеродные нанотрубки (ОУНТ) и многостенные углеродные нанотрубки (МУНТ), на величину математического ожидания и дисперсии коробления пластин из волокнистого композиционного материала. Были рассмотрены ламинаты с дезориентацией волокон как асимметричные, и для оценки коробления использовали модель, предложенную Dano и Hyer. Полученные результаты подтверждают, что добавление углеродных наночастиц в качестве модификатора в полимерную матрицу волокнистого композиционного материала позволяет увеличить размеростабильность (математическое ожидание среднеквадратичного отклонения (СКО)) и технологическую устойчивость схемы армирования (дисперсия выборки СКО композиционной пластины). Математическое моделирование коробления пластины с учетом возможной дезориентации волокна показало снижение дисперсии коробления на 12,6 и на 26,6 % при модификации ОУНТ и МУНТ соответственно. Экспериментально определены коэффициент линейного термического расширения (КЛТР) наноструктурированной полимерной матрицы с различными наполнителями. Обнаружено, что углеродные наномодификаторы более эффективны как компенсаторы термического расширения полимерной матрицы в композиционных материалах, армированных углеродными волокнами, чем в полимерной матрице без макроволокон. Добавление 0,05 % УНТ, 1 % МУНТ в эпоксидную смолу позволяет снизить КЛТР на 9,7 и 15,4 % соответственно. В то же время добавление аналогичного количества наночастиц в полимерную матрицу волокнистого композиционного материала снижается КЛТР поперек волокон на 15,56 и 35,8 % соответственно. На основании полученных результатов были построены зависимости КЛТР в трансверсальном направлении полимерного композиционного материала, математическое ожидание СКО и дисперсия выборки СКО точности формы композиционной пластинки от концентрации модификатора. На основании полученных данных можно сделать вывод, что для снижения математического ожидания и дисперсии коробления композиционного материала существует эффективная концентрация, увеличение которой нецелесообразно, несмотря на дальнейшее снижение КЛТР в трансверсальном направлении.

© **Обверткин Иван Владимирович** – н.с., e-mail: +79632609742@yandex.ru, ID: 0000-0003-4895-5757.
Пасечник Кирилл Арнольдович – н.с., e-mail: pasechnik.kirill@gmail.com, ID: 0000-0001-6245-1630.
Власов Антон Юрьевич – к.ф.-м.н., доц., e-mail: vlasov.anton@gmail.com, ID: 0000-0002-6360-7382.

Ivan V. Obvertkin – Researcher, e-mail: +79632609742@yandex.ru, ID: 0000-0003-4895-5757.
Kirill A. Pasechnik – Researcher, e-mail: pasechnik.kirill@gmail.com, ID: 0000-0001-6245-1630.
Anton Yu. Vlasov – CSc in Physical and Mathematical Sciences, Associate Professor,
e-mail: vlasov.anton@gmail.com, ID: 0000-0002-6360-7382.

THE POTENTIAL OF USING SWCNTS, MWCNTS AND CNFS CAPABLE OF INCREASING THE COMPOSITE MATERIAL DIMENSIONAL AND TECHNOLOGICAL STABILITY AS MODIFIERS OF A POLYMER MATRIX

I.V. Obvertkin, K.A. Pasechnik, A.Y. Vlasov

Reshetnev Siberian State University of Science & Technology, Krasnoyarsk, Russian Federation

ARTICLE INFO

Received: 04 May 2021
Accepted: 10 December 2021
Published: 30 December 2021

Keywords:

Nanocomposites, Carbon nanotubes and nanofibers, Thermomechanical characteristics, Analytical modeling, Thermal analysis.

ABSTRACT

In this study, the effect of carbon nanofibers (CNN), single-wall carbon nanotubes (SWCNTs) and multi-wall carbon nanotubes (MWCNTs) on the warpage expected value and warpage dispersion of a plate made of a fibrous composite material are investigated. Laminates with fiber disorientation were considered as asymmetric and the model proposed by Dano and Hyer was used to evaluate the warpage. The results obtained confirm that the addition of carbon nanoparticles as a modifier to the polymer matrix of a fibrous composite material can increase the dimensional stability (the mathematical expectation of the standard deviation) and the technological stability of the reinforcement scheme (the variance of the standard deviation of the composite plate). Modeling of the warpage of plate, taking into account the possible disorientation of the fiber, showed a decrease in the warpage dispersion by 12.6 and 26.6 % with the modification of the SWNTs and MWCNTs, respectively. The coefficient of thermal extension (CTE) of a nanostructured polymer matrix with various fillers were experimentally determined. It was found that carbon nanomodifiers are more effective as compensators for the thermal expansion of the polymer matrix in composite laminates reinforced with carbon fibers than the polymer matrix without macrofibers. The addition of 0.05 % SWCNTs, 1 % MWCNTs to the epoxy resin reduces the CTE by 9.7 and 15.4 %, respectively. At the same time, the addition of a similar amount of nanoparticles to the epoxy matrix of the fiber composite reduces the CTE in the transverse direction by 15.56 and 35.8 %, respectively. On the basis of the obtained results, the dependences of the transverse CTE of the polymer composite material, the mathematical expectation of the standard deviation, and the variance of the standard deviation of the composite plate form accuracy on the concentration of the modifier were constructed. According to the obtained data, it can be concluded that in order to reduce the mathematical expectation and the variance of the warping of the composite material, there is an effective concentration, the increase of which is impractical, despite the further decrease in the transversal CTE.

Introduction

Continuous demand for light weight, cost-effectiveness, high strength, dimensional stability and accuracy of products from polymer-matrix composites (PMCs) is the driving force behind the search for new materials. The discovery of carbon fillers made it possible to make a quantum leap in the creation of nanocomposites. Carbon nanoparticles such as nanotubes and nanofibers are materials with a unique structure and an unusual combination of properties, such as high strength and flexibility, high Young's modulus and a negative CTE [1–11]. The unique properties of materials allow them to be highly effective modifiers for polymer matrices directionally changing their mechanical and thermomechanical characteristics [9, 12, 13].

The paper investigates the effect of carbon modifiers on the warpage of the composite material. Modifiers have a high Young's modulus, a low CTE and high polymer-modifier affinity. The hypothesis of increase in the technological stability of composite material reinforcement schemes when using modified resin is also tested. In addition, it is necessary to pay attention to the change in technological properties of modified polymer matrix, in particular, to the study of their rheology, as well as to the extent of the effect of nanoparticles dispersion and morphology on the rheology of the polymer material. The dispersion rheology plays an important role in nanocomposites processing due to the large increase in the system viscosity with increasing of the nanomodifier concentration [11–40].

For the first time in history, polymer nanocomposites were studied in [25]. Since then, there have appeared many works devoted to the manufacture and study of the properties of polymer nanocomposites. The authors of the study [41] investigated the modification of epoxy resin with multilayer nanotubes aligned in a magnetic field, and they succeeded in reducing the CTE of the epoxy resin by 11.6 % with random distribution of the modifier and by 12.6 and 10.8 % in the direction of alignment and perpendicular to the direction of alignment in a magnetic field, respectively. The authors of [23] also studied the effect of the volume fraction of MWCNTs on the nanocomposite CTE. They determined that the nanocomposite CTE tends to decrease with increase in the volume fraction of carbon nanotubes. The CTEof composites containing 0 (epoxy resin), 8.5, 10.4, 14.1, 21.2, and 27.0 volume % of MWCNTS is $7.0 \cdot 10^{-5}$; $0.4 \cdot 10^{-5}$; $-0.6 \cdot 10^{-5}$; $-1.4 \cdot 10^{-5}$; $-0.5 \cdot 10^{-5}$ and $-0.7 \cdot 10^{-5}$, respectively. It was shown in [42] that the addition of 1 % of carbon nanofibers into epoxy resin increases Young's modulus and flexural strength by 26 and 20 %, respectively, and decreases the nanocomposite CTE by

53 %. The authors of [1] were able to increase Young's modulus by 11 % and decrease the CTE by 32.5 % adding 1 percent of carbon nanofibers for weight (length 30 microns, diameter 20–80 nanometers) into epoxy resin. The authors of [13] were able to increase Young's modulus by 9 % and decrease the CTE of the nanocomposite by 23.7 % adding 1 percent of MWCNTs for weight (length 0.5–2 microns, diameter 8–15 nanometers) into epoxy resin.

Another important factor in the effectiveness of the modifier is the interfacial interaction between the nanofiller and the epoxy matrix. Numerous methods such as functionalization of nanofillers, ultrasonic treatment, and homogenization are used in an attempt to improve bond strength or interfacial adhesion. It was found that the agglomeration of carbon nanoparticles dramatically reduces the mechanical properties of the fabricated nanocomposites. Because of the small size and high aspect ratio of nanoparticles, individual carbon nanoparticles are usually twisted and therefore do not exhibit as high efficiency as possible. Therefore, without effective dispersion and establishment of strong chemical affinity with the polymer matrix, it is impossible to transfer the properties of carbon nanoparticles to the finished product. Although, according to the data of researchers [26], the functionalization of carbon nanotubes reduces their mechanical properties.

At the macrolevel the classical lamination theory (CLT) is most often used to assess the emerging macrostresses in laminated composites [29]. This theory also makes it possible to predict the shape of laminates after curing. It is although important to remember that the classical lamination theory has a number of limitations, in particular, it does not take into account such important factors as the effect of the cooling rate and changes in the matrix properties during the curing process [28].

To assess the stresses arising in a polymer composite, several theories are used, such as elasticity solution [30–32], cylinder theory [33–50], Eshelby theory [39] and energy method [40]. The Mori-Tanaka's model [51, 57, 54] is used in this work to assess the effective elastic properties of the polymer matrix reinforced with nanoparticles [54–71]. CLT is used to assess the effective elastic properties of the composite. The models [58, 71] are used to assess CTE of composite.

Modeling of the warpage of composite material taking into account the fibers disorientation was carried out in [73, 74]. To assess the shape of composite materials the authors of [73] use CLT with the assumption that the structure of the material with disorientated layers will be close to a symmetric one. In [74] the finite element method was used to model the laminate shape. In this paper we consider disorientated laminates as asymmetric ones and use the model proposed by Dano and Hyer [61].

Previous studies have shown that reducing the warpage of the composite material can be achieved through the use of nanomodifiers. But none of the previous works, as far as the authors know, experimentally studied the effect of nanoadditives on the technological stability of reinforcement schemes.

In this paper, we consider composite laminates with quasi-isotropic reinforcement schemes, which have theoretically near zero warpage, due to the fact that the thermal stresses in these materials are balanced. However, the presence of reinforcing fibers disorientation causes to warpage. Modification of the polymer matrix in order to reduce the difference between the thermomechanical properties of the components allows to reduce the effect of fiber disorientation on the dimensional stability and technological stability. The purpose of this study is to study the effect of carbon nanomodifiers on dimensional stability as the mathematical expectation of the standard deviation of the composite plate form accuracy and technological stability as the variance of the standard deviation of the composite plate form accuracy, taking into account the disorientation of reinforcing fibers. The influence of the selected modifiers on the viscosity of the epoxy matrix, depending on the concentration and functionalization, is also studied. The functionalization was performed to add functional oxygen-containing groups to the surface of the modifier.

1. Experimental procedure

1.1. Materials

Manufactured by "INUMIT" CJSC two-component epoxy system T67 containing a mixture of epoxy resins based on bisphenol A and epichlorohydrin as well as aromatic and aliphatic diamines was used as the modified resin.

TUBALL ™ SWCNTs from OCSiAl company with an average outer diameter of 1.6 ± 0.4 nm and length of more than 5 μm [5], multi-walled carbon nanotubes of the "Taunit" series of the Nanotech Center LLC with an outer diameter of 20–50 nm and length of more than 2 μm [45], as well as carbon nanofibers from 50 to 250 nm with fiber length of up to 0.5 mm obtained at the Institute of Catalysis named after G.K. Boreskov SB RAS, Russia [46] were used as modifiers of the polymer matrix in this work. A comparative overview of various carbon nanomodifiers is given in Table 1.

Table 1

Review of the characteristics of carbon nanomodifiers

Property	MWCNTs	SWCNTs	CNFs
Diameter (nm)	5–50 [14]; 13–36 [17,18]; 12,5 [8]	0.6–0.8 [14]; 1,6 ± 0,4 [3,4,5,7]	50–200 [19,20]
Length (μm)	1,8–10,99 [1718]	5 [3,4,5]	100 [19,20]
Young's modulus (GPa)	1000 [14]; 270–970 [17, 18]; 800 [8]; 1280 [21]	1500 [14]; 790 [7]	240 [6]
Tensile strength (GPa)	10–60 [15]; 63 [22]	50–500 [15]	2.92 [19,20]
CTE	$-1{,}2\cdot10^{-5}$ [23]; $-1{,}02\cdot10^{-5}$; $-0{,}72\cdot10^{-5}$ [10]	$-2\cdot10^{-5}$[24]	$-0{,}41\cdot10^{-6}$ [1]; $-1\cdot10^{-6}$[2]
Thermal conductivity (W/m·K)	3000–6000 [16]	3000–6000 [16]	1950 [19,20]

Table 2

Properties of materials used to calculate the properties of modified epoxy resin and composite materials based on it.

Material	Physical and mechanical properties	Thermomechanical properties
Epoxy resin T67	Young's modulus, GPa: E_m = 3.17 [65] Poisson's ratio: ν_m = 0.35 [67]	CTE: $\alpha_m = 68 \cdot 10^{-6}$
Carbon fibersK500	Young's modulus, GPa: E_{1f} = 436 [70]; E_{2f} = 14 [71]; E_{3f} = 14 [71] Poisson's ratio: ν_{12f} = 0.2 [67]; ν_{23f} = 0.46 [73]; ν_{13f} = 0.2 [67] Shear modulus, GPa: G_{12f} = 8.78 [64]; G_{23f} = 2.1; G_{13f} = 8.78 [64]	CTE: $\alpha_{1f} = -0.9 \cdot 10^{-6}$; $\alpha_{2f} = 6.8 \cdot 10^{-6}$[63, 66]
Carbon fibers IMS65	Young's modulus, GPa: E_{1f} = 290 [68]; E_{2f} = 21.8 [64]; E_{3f} = 21.8[64]. Poisson's ratio: ν_{12f} = 0.2 [67]; ν_{23f} = 0.46 [69]; ν_{13f} = 0.2[67] Shear modulus, GPa: G_{12f} = 12.5[64]; G_{23f} = 8.2; G_{13f} = 12.5[64].	CTE: $\alpha_{1f} = -0.56 \cdot 10^{-6}$ [70]; $\alpha_{2f} = 10 \cdot 10^{-6}$ [66]
MWCNT	Young's modulus, GPa: E_f = 1000 [14] Poisson's ratio: ν_{f12} = 0.2[56]	CTE: $\alpha_f = -1.2 \cdot 10^{-5}$ [23]
SWCNT	Young's modulus, GPa: E_f = 1500 [13] Poisson's ratio: ν_{f12} = 0.2[54]	CTE: $\alpha_f = -2 \cdot 10^{-5}$ [24]

Some properties of the materials presented in the table 2 were directly measured in the course of the work, some information was provided by the manufacturers of materials, and some data was taken from the research of other authors who studied these materials or materials with similar properties.

Carbon fibers IMS 65 are presented in the form of spread tow fabric. Carbon fiber is spread to a 25 mm width tape. The fabric has arranging the fibers in the woven structure in the straightest orientation possible the fiber properties are used in the most effective way. Due to fabric can presented as two unidirectional orthotropic layers.

1.2. Equipment and research methods

The researched carbon nanoparticles were functioned to increase the polymer-modifier affinity.

To increase the adhesion between carbon nanoparticles, functionalization was performed to add functional oxygen-containing groups to the surface of the modifier. Two methods were used in this work for the functionalization of nanoparticles.

According to the first method, the classical Hammers oxidation method was used to modify the surface with the addition of functional oxygen-containing groups [43, 44]. 400 ml of concentrated sulfuric acid containing 2.5 g of ammonium nitrate was gradually added into a round bottom flask containing 5 g of carbon nanotubes. After stirring for 20 minutes, 1.5 g of potassium permanganate was added to the ice baths while the temperature did not rise, and the mixture was stirred for an additional 20 minutes. Then the temperature of the mixture was gradually increased to 40 °C and held for 30 minutes. Then 700 ml of deionized water was successively added stirring and kept for 15 minutes. Then the suspension was treated with hydrogen peroxide until the appearance of a yellowish hue and the absence of exothermic reaction. The resulting suspension was then treated with ion exchange resins, filtered and washed with a total of 7 liters of distilled water. The resulting modified nanotubes were dried on calcium chloride and silica gel.

The second method included holding at 35 °C for 7 days in methylene chloride under reflux. Then carbon nanoparticles were sonicated in a water bath in concentrated sulfuric and nitric acid in a ratio of 3 to 1 for 3 hours after filtration in vacuum and washing with distilled water. Then carbon nanoparticles were collected and dried on calcium chloride and silica gel.

The IR spectra of functionalized and native nanotubes were measured using a NicoletiS10 FT-IR spectrometer (ThermoFisherScientific) in the range of wave numbers 400–4000 cm^{-1}. Before measurements the samples were dried at the temperature of 120 degrees for 12 hours to remove traces of water. The measurement of carbon nanotubes was carried out in mixture with KBr at room temperature.

Images of carbon nanotubes were obtained using a Hitachi HT7700 transmission electron microscope.

The researched nanocomposites modified with various carbon nanoparticles were made using sonication technology. First the epoxy resin was mixed for 30 minutes at 2000 rpm. Then the mixture was treated with ultrasound (UZDN-A, kHz 22 ± 1.65) for 40 minutes, with a pause every five minutes to cool the mixture. During cooling the container with the mixture was immersed in water. After completion of the sonication a hardener was added to the mixture and stirred for 10 minutes. Then air bubbles were removed by degassing the mixture in vacuum for 5 minutes. Then the mixture was cured at the temperature of 80 °C for 3 hours and at the temperature of 120 °C for 6 hours.

The viscosity of the resulting mixture after the degassing process was determined on a Discovery Hybrid Rheometers (DHR - 2) rotary rheometer at the constant mixture temperature of 50 degrees and with increasing a shear rate up to 16.4 s^{-1}.

Samples of a polymer composite material based on modified resin were obtained using the method of vacuum

assisted resin infusion molding (VARIM). Metal tooling was coated with a release agent. Dry carbon fabric was laid out according to the reinforcement scheme. After laying out the required number of patterns, the release fabric was laid out, and the resin supply and discharge lines are installed on the distribution grid. Next, a vacuum bag was formed, connected to a vacuum pump and degassed for 1 hour at the temperature of 50 °C. The epoxy resin was mixed in stoichiometric ratio of 100 / 40.9 resin / hardener. After that, the reinforcing material is impregnated with resin. Then the tooling with impregnated reinforcing materials is cured in vacuum at the temperature of 80 °C for 3 hours and at the temperature of 120 °C for 6 hours.

After the curing process, the CTE of the manufactured samples was determined using a TAInstrumentsQ400 thermomechanical analyzer. The tests were carried out with constant heating to 100 °C at a constant heating rate of 5 °C/min. At least three samples are used for each fillers concentration.

The volume ratio of the reinforcing element in the composite material was determined using a Discovery TGA55 TA Instruments thermogravimetric analyzer (USA).

The flatness of the sample surface was measured using an Absolute Arm 7520 SE portable coordinate measuring machine with an external CMS 108 scanner with Geomagic software (Romer) with a spatial accuracy of ± 0.033 mm.

2.3. Mathematical modeling of the effect of modification with carbon nanotubes on the physical and thermomechanical characteristics of the composite material

The Mori-Tanaka's method was used to estimate the CTE of the modified epoxy resin [51, 52]. Elements of the Eshelby Tensor for inclusions with an aspect ratio tending to infinity are given in [53]. Expressions for calculating the effective CTE of the modified epoxy resin are given in Appendix 1. Expressions for calculating the effective Young's modulus of the modified polymer matrix are given in Appendix 1. The calculations were based on the characteristics of the materials shown in Table 2.

Mathematical modeling of the effect of modification with carbon nanotubes on the mathematical expectation of the standard deviation of warpage.

Estimation of the mean standard deviation of warpage is performed according to the model for predicting the shape of an asymmetric composite material sample proposed by Dano and Hyer [60, 61], based on polynomial approximation of displacements, extending CLT including geometric nonlinearity and using the Rayleigh-Ritz method to minimize the total potential energy. The description of the model is briefly presented below.

Total potential energy of laminate W:

$$W = \int_{vol} \omega d(vol). \tag{1}$$

Where ω is strain energy density.

$$\omega = \frac{1}{2} C_{ijkl} \varepsilon_{ij} \varepsilon_{kl} - \alpha_{ij} \varepsilon_{ij} \Delta T. \tag{2}$$

Where C_{ijkl} are elastic constants, ε_{ij} and ε_{kl} are strains, α_{ij} is the CTE, ΔT is the difference between strees-free and current temperatures as $\Delta T = 95$ ºC. Stress-free temperature is maximum curing temperature equal to 120 ºC. Current temperature is 25 ºC.

CLT implies a plane stress strain state, that is, normal stresses in the z direction and shear stresses not in the plane of the laminate are assumed to be zero, resulting in the following expression for the total potential energy:

$$\begin{aligned} W = \int_{-\frac{Lx}{2}}^{\frac{Lx}{2}} \int_{-\frac{Ly}{2}}^{\frac{Ly}{2}} \int_{-\frac{H}{2}}^{\frac{H}{2}} \frac{1}{2} Q_{11} \varepsilon_x^2 + Q_{12} \varepsilon_x \varepsilon_y + Q_{16} \varepsilon_{xy} \varepsilon_x + \frac{1}{2} Q_{22} \varepsilon_y^2 + \\ + Q_{26} \varepsilon_{xy} \varepsilon_y + \frac{1}{2} Q_{66} \varepsilon_{xy}^2 - \left(Q_{11} \alpha_x + Q_{12} \alpha_y + Q_{16} \alpha_{xy} \right) \varepsilon_x \Delta T - \\ - \left(Q_{12} \alpha_x + Q_{22} \alpha_y + Q_{26} \alpha_{xy} \right) \varepsilon_y \Delta T - \\ \left(Q_{16} \alpha_x + Q_{26} \alpha_y + Q_{66} \alpha_{xy} \right) \varepsilon_{xy} \Delta T dz dy dx. \end{aligned} \tag{3}$$

Where Q_{ij} are components of the stiffness matrix of each layer, Lx and Ly are sample width and length, H is total laminate thickness. The strain components ε_x, ε_y and ε_{xy} are determined by the expressions:

$$\varepsilon_x = \varepsilon_x^0 + z k_x, \tag{4}$$

$$\varepsilon_y = \varepsilon_y^0 + z k_y, \tag{5}$$

$$\varepsilon_{xy} = \varepsilon_{xy}^0 + z k_{xy}. \tag{6}$$

The quantities ε_x^0, ε_y^0, ε_{xy}^0 и k_x, k_y, k_{xy} are the deformation of the middle surface and the curvature, respectively, determined by expressions that take into account geometric nonlinearity in accordance with the theory of von Karman:

$$\varepsilon_x^0 = \frac{\partial u^0}{\partial x} + \frac{1}{2} \left(\frac{\partial w^0}{\partial x} \right)^2, \tag{7}$$

$$\varepsilon_y^0 = \frac{\partial v^0}{\partial y} + \frac{1}{2} \left(\frac{\partial w^0}{\partial y} \right)^2, \tag{8}$$

$$\varepsilon_{xy}^0 = \frac{\partial u^0}{\partial y} + \frac{\partial v^0}{\partial x} + \frac{\partial w^0}{\partial x} \frac{\partial w^0}{\partial y}, \tag{9}$$

$$k_x = -\frac{\partial^2 w^0}{\partial x^2} = -a, \tag{10}$$

$$k_y = -\frac{\partial^2 w^0}{\partial y^2} = -b, \tag{11}$$

$$k_{xy} = -2 \frac{\partial^2 w^0}{\partial x \partial y} = -c. \tag{12}$$

According to the work of Dano and Hyer, the components of the middle surface deformation can be approximated by polynomials of the third order, consisting of the terms the sum of the powers x and y of which is an even number:

$$\varepsilon_x^0 = d_1 + d_2 x^2 + d_3 xy + d_4 y^2, \quad (13)$$

$$\varepsilon_y^0 = d_5 + d_6 x^2 + d_7 xy + d_8 y^2, \quad (14)$$

$$\varepsilon_{xy}^0 = 2d_9 + \left(ab - \frac{c^2}{4} + 2d_4 + 2d_6 \right) xy + \\ + \left(\frac{1}{2}\left(\frac{ac}{2} + d_3 \right) + d_{10} \right) x^2 + \left(\frac{1}{2}\left(\frac{bc}{2} + d_7 \right) + d_{11} \right) y^2. \quad (15)$$

Substituting expressions (13), (14), (15) into equation (3), we obtain the equation of the total potential energy in the form of a function of 14 unknowns:

$$W = W\left(a,\ b, c, d_1, d_2, d_3, d_4, d_5, d_6, d_7, d_8, d_9, d_{10}, d_{11}\right) \quad (16)$$

To ensure a state corresponding to the minimum potential energy, it is necessary:

$$\partial W = \sum_{i=1}^{14} \frac{\partial W}{\partial x_i} \partial x_i = 0. \quad (17)$$

Where x_i – $a,\ b, c, d_1, d_2, \ldots, d_{11}$. To ensure condition (17), it is required:

$$f_i = \frac{\partial W}{\partial x_i} = 0, \quad (18)$$

where i = 1, 2, … 14. This leads to a system of 14 nonlinear equations with 14 unknown constants x_i, the solution of which makes it possible to find the sample shape of an asymmetric composite material. By sequential execution of simple algebraic transformations the system of nonlinear equations is reduced to a system of 3 nonlinear equations with three unknown constants $a,\ b, c$. The Newton-Raphson method is used to solve the system. The method requires specifying an initial approximation. The found solution will depend on the choice of this approximation, especially if the sample under consideration has more than one stable shape, for example, bistable samples can have two stable shapes and unstable one [62]. The resulting solution is stable in the case of a positive definite Jacobi matrix:

$$J = \frac{\partial\left(f_1, f_2, \ldots f_{14}\right)}{\partial\left(a, b, \ldots d_{11}\right)}. \quad (19)$$

The displacement of the analyzed sample points in the *z* direction is assumed to be:

$$w(x, y) = 0{,}5\left(ax^2 + by^2 + cxy\right). \quad (20)$$

The standard deviation of warpage:

$$s = \sqrt{\frac{1}{N-1} \sum_{l=1}^{N} \left(w_l - w'\right)^2}, \quad (21)$$

where $l = 1 \ldots N$ is the number of control points on the sample; x and y are coordinates of control points; w_l is warpage at control point l; w' is the arithmetic mean for a sample of N points.

The mathematical expectation of the standard deviation of warpage is:

$$E[s] = \sum_{i=1}^{n} s_i \cdot P_i, \quad (22)$$

where s_i is the standard deviation of warpage with the angles of layers disorientation corresponding to the i design case; P_i is the probability value corresponding to the i design case. The number n corresponds to the number of placements $\overline{A}_m^k = m^k$, where k is the number of layers in the sample, m is the number of discrete steps $\Delta\theta'$ in the range from $-\theta'$ to $+\theta'$ of the expected maximum disorientation angle. The probability P_i is equal to the product of the values of the probability P_{ij} $(j = 1 \ldots k)$ of the disorientation occurrence within the boundaries of the discrete step $\Delta\theta'$ of each layer.

The value of the probability P_{ij} is determined using the equation for the normal distribution law:

$$P_{ij} = \int_a^b \frac{1}{s_{\theta'}\sqrt{2\pi}} e^{\frac{-\left(\theta_{ij} - \mu\right)^2}{2 s_{\theta'}^2}} \quad (23)$$

Where a and b are the boundaries of the discrete step $\Delta\theta'$; $\sigma_{\theta'}$ is standard deviation of the distribution; μ is the mathematical expectation of the distribution. In view of the previously accepted θ' as the range of possible disorientation, we will write $3\sigma_{\theta'} \approx \theta'$; μ is taken equal to 0.

For each possible combination of disorientation angles we determine the curvature parameters k_x, k_y and k_{xy} using the Dano and Hyer model. Next, we determine the probability density function $p(\sigma)$ of the deviation of warpage, the true functions of which are continuous. Due to the finite number of calculated values of σ, we set a discrete range $\Delta\sigma$ and summarize the values of the probabilities included in the ranges of calculated cases.

The numerical solution was performed in the Python software environment according to the presented equations.

2. Results and Discussion

FTIR spectra of native and functionalized carbon nanoparticles shown in Figure 1 were obtained. The spectra contain intense bands at 3431 cm^{-1} (stretching vibrations of the –OH group), which can be attributed to hydroxyl groups

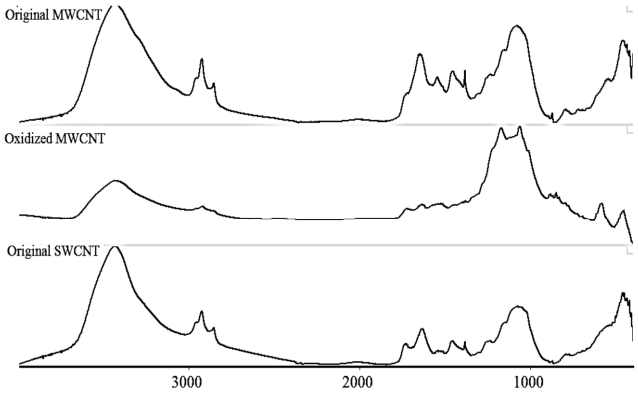

Fig. 1. FTIR spectra of native and functionalized CNTs

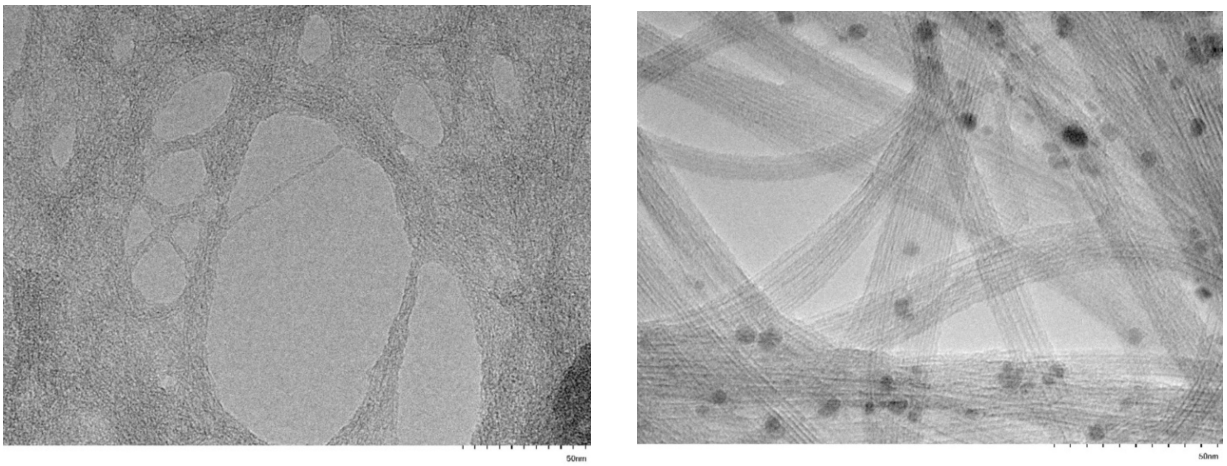

Fig. 2. Image of functionalized (left) and native (right) single-walled carbon nanotubes

and to a trace of water in the potassium bromine tablet used for analysis. The bands at 1724 and 1736 cm^{-1} probably corresponding to C = O were attributed to stretching vibrations of carboxylic acid groups (–COOH). The bands in the 1250–950 cm^{-1} range are probably related to the vibration of the C–O bond in a different chemical environment. The relative increase and partial separation of the bands in this wave region indicate increase in the number of surface oxygen-containing functional groups [57], which provide electrostatic and chemical interaction of carbon nanoparticles with a polymer matrix, allowing more uniform distribution in the volume.

However, a high degree of functionalization causes the appearance of a large number of defects in graphene layers, especially in single-walled nanotubes. Figure 2 shows images of functionalized and native carbon nanotubes, which demonstrate the absence of the structure inherent in nanotubes after their modification.

The viscosity of epoxy systems was investigated at various concentrations of modifiers. The epoxy resin has distinct pseudoplastic behavior with decreasing viscosity whenthe shear rate increases. When carbon nanoparticles are added, the viscosity of the mixture increases. This effect is most noticeable at low shear rates, and is partially offset by increasing shear rates. These changes can be explained by the formation of a randomly distributed percolationnetwork. Organized structures are destroyed at high shear rates, which makes it possible to reduce the viscosity due to the alignment of modifiers in the direction of flow [47]. Different tendency of modifiers to form a percolation network explains their different effect on the dispersion viscosity. Native single-walled carbon nanotubes are characterized by the greatest influence on the viscosity of the modified resin from the studied materials, functionalized multi-walled nanotubes are characterized by the least one.

Figure 3 shows the dependence of the modified epoxy resin viscosity on the concentration of carbon nanotubes or nanofibers measured at a constant mixture temperature of 50 degrees. As it can be seen from image 3, even at high concentration of functionalized MWCNTs the dispersion viscosity is low and suitable for processing by such methods as vacuum infusion and injection molding. Sharp increase in viscosity with increase in the concentration of native CNTs is explained by the fact that at a given concentration a percolation network is formed. The network prevents the mobility of the polymer chain, which leads to increase in viscosity [48–50]. As Figure 3 shows, functionalized SWCNTs have less effect on the rheology of the modified resin, which may be due to their greater tendency to agglomeration and destruction of the SWCNT structure upon modification. Agglomerating into large formations, nanomodifiers reduce their effective amount in the polymer matrix. To introduce functionalized SWCNTs into the resin, we used the “Solution processing” method [47], since after the drying stage the CNTs are not dispersed into the polymer matrix during the functionalization of their surfaces by the Hammers method. The addition of CNFs into the polymer matrix does not significantly affect its rheological properties, regardless of the CNFs functionalization. At CNFs concentration of 10 %, the viscosity of the mixture reaches 0.45 Pa×s.

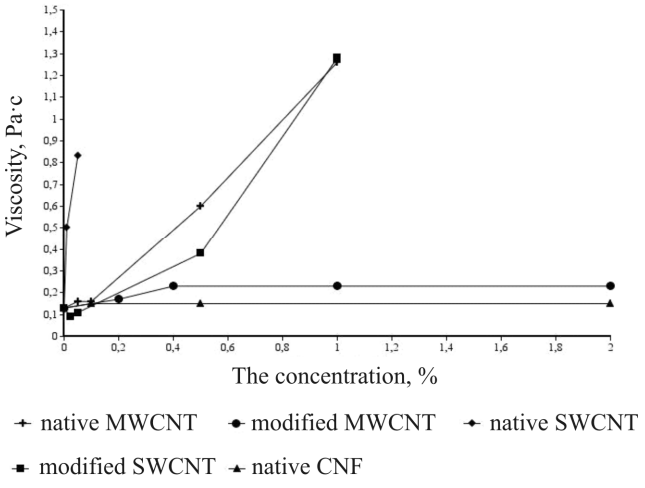

Fig. 3. Influence of the carbon nanoparticles concentration on the viscosity of the modified resin

We made samples of the modified resin with various functionalized and native fillers. The effect of modifica-

tion with various carbon nanoparticles on the CTE of the binder is shown in Table 3. Multi-walled nanotubes modified by the second method turned out to be the most effective. At the concentration of 1 %, they reduce the CTE of the polymer matrix by 15.4 %. Native SWCNTs reduce the CTE of epoxy resin by 9.7 % at the concentration of 0.05 %.

Native SWCNTs and functionalized MWCNTs were used as the most effective modifiers for further research. Table 4 shows the measured and calculated values for the selected modifiers.

Samples of fibrous polymer composite material based on unidirectional carbon fibers and modified and unmodified epoxy resin were made. The fiber volume fraction in the unidirectional composite material was determined using thermogravimetric analysis. The CTE of the material across and along the carbon fibers was measured. The results are presented in Table 5.

The calculated data obtained from the research using the models [59, 72] showed high convergence with the measured data. To assess the convergence of the calculated and measured CTE values in the transverse direction, we used the values measured out-of-plane of the sample in order to neutralize the possible effect of fiber disorientation during the sample manufacture.

Taking into account the possible disorientation of fibers in the plane, mathematical modeling of the warpage of plate was carried out on the basis of the properties presented in the table 6. The CLT was used to estimate the effective elastic properties of the composite. The models described in [59, 72] were used to estimate the effective CTE of the composite. The samples were made of spread tow fabric based on carbon fiber IMS 65 and unmodified or modified epoxy resin and have a reinforcement scheme [0/60/–60]. The samples have thickness 0.24 mm and the size of plate in the XY plane: 200×200 mm.

Table 3

Influence of carbon nanoparticles on the epoxy resin CTE

Modifier	The most effective concentration, %	CTE of modified resin (reduction relative to pure resin)
Native CNFs	4	$64{,}09\cdot10^{-6}$ (7,1 %) ± $1{,}71\cdot10^{-6}$
Functionalized CNFs	4	$63{,}10\cdot10^{-6}$ (8,6 %) ± $1{,}53\cdot10^{-6}$
Native SWCNTs	0,05	$62{,}3\cdot10^{-6}$ (9,7 %) ± $1{,}64\cdot10^{-6}$
Functionalized SWCNTs	0,05	$64{,}61\cdot10^{-6}$ (6,3 %) ± $0{,}95\cdot10^{-6}$
Native MWCNTs	1	$67{,}98\cdot10^{-6}$ (1,4 %) ± $1{,}42\cdot10^{-6}$
Functionalized MWCNTs	1	$58{,}37\cdot10^{-6}$ (15,4 %) ± $0{,}78\cdot10^{-6}$

Table 4

Characteristics of CNT-modified epoxy resin

Test sample	Measured CTE, C^{-1}	Predictive CTE, C^{-1}	Predictive Young's modulus, E_m GPa
T67+0,01 % non-functionalized SWCNTs	$66{,}99\cdot10^{-6}\pm1{,}59\cdot10^{-6}$	$66{,}83\cdot10^{-6}$	3,281
T67+0,05 % non-functionalized SWCNTs	$62{,}3\cdot10^{-6}\pm1{,}64\cdot10^{-6}$	$62{,}96\cdot10^{-6}$	3,72
T67+0,2 % functionalized MWCNTs	$65{,}02\cdot10^{-6}\pm1{,}7\cdot10^{-6}$	$58{,}19\cdot10^{-6}$	3,879
T67+0,4 % functionalized MWCNTs	$63{,}83\cdot10^{-6}\pm1{,}57\cdot10^{-6}$	$53{,}58\cdot10^{-6}$	4,539
T67+1 % functionalized MWCNTs	$58{,}37\cdot10^{-6}\pm0{,}78\cdot10^{-6}$	$47{,}84\cdot10^{-6}$	6,414
T67+2 % functionalized MWCNTs	$61{,}53\cdot10^{-6}\pm0{,}56\cdot10^{-6}$	$44{,}43\cdot10^{-6}$	9,478

Table 5

Properties of unidirectional composite material

Indicators	Unidirectional layer of composite based on carbon fiber k500 (Fiber volume fraction 57 %)					
	T67		T67+0,05 % unmodified SWCNTs		T67+1 % modified MWCNTs	
	Calculation	Measurement	Calculation	Measurement	Calculation	Measurement
Longitudinal CTE, α_1 C^{-1}	$-0{,}52\cdot10^{-6}$	$-1{,}192\cdot10^{-6}\pm0{,}26\cdot10^{-6}$	$-0{,}492\cdot10^{-6}$	$-1{,}197\cdot10^{-6}\pm0{,}21\cdot10^{-6}$	$-0{,}365\cdot10^{-6}$	$-1{,}10\cdot10^{-6}\pm0{,}28\cdot10^{-6}$
Change in the indicator relative to composite with unmodified resin, %	–		–0,38180		7,85	
Transverse CTE, α_2 C^{-1}	–	$33{,}575\cdot10^{-6}\pm1{,}61\cdot10^{-6}$	–	$26{,}572\cdot10^{-6}\pm1{,}26\cdot10^{-6}$	–	$21{,}43\cdot10^{-6}\pm0{,}19\cdot10^{-6}$
Change in the indicator relative to composite with unmodified resin, %	–		20,85		36,17	
Out-of-plane, α_3 C^{-1}	$38{,}81\cdot10^{-6}$	$42{,}735\cdot10^{-6}\pm1{,}25\cdot10^{-6}$	$35{,}82\cdot10^{-6}$	$36{,}083\cdot10^{-6}\pm1{,}79\cdot10^{-6}$	$27{,}39\cdot10^{-6}$	$27{,}435\cdot10^{-6}\pm1{,}14\cdot10^{-6}$
Change in the indicator relative to composite with unmodified resin, %	–		15,56		35,8	

Table 6

Properties of an elementary layer of composite material

Indicators	Layer of composite based on carbon fiber IMS65 (Carbon fiber content 47 %)		
	T67	T67+0,05 % unmodified CNFs	T67+1 % modified MWCNTs
Longitudinal modulus, E_1,GPa	138.55	138.84	140.27
Transverse modulus, E_2,GPa	11.96	12.25	13.68
In-plane shear modulus, G_{12},GPa	4.44	4.88	6.24
Major Poisson's ratio, ν_{12}	0.279	0.273	0.251
Longitudinal CTE, α_1, C^{-1}	$0.268 \cdot 10^{-6}$	$0.339 \cdot 10^{-6}$	$0.608 \cdot 10^{-6}$
Transverse CTE, α_2, C^{-1}	$48.57 \cdot 10^{-6}$	$44.83 \cdot 10^{-6}$	$34.19 \cdot 10^{-6}$

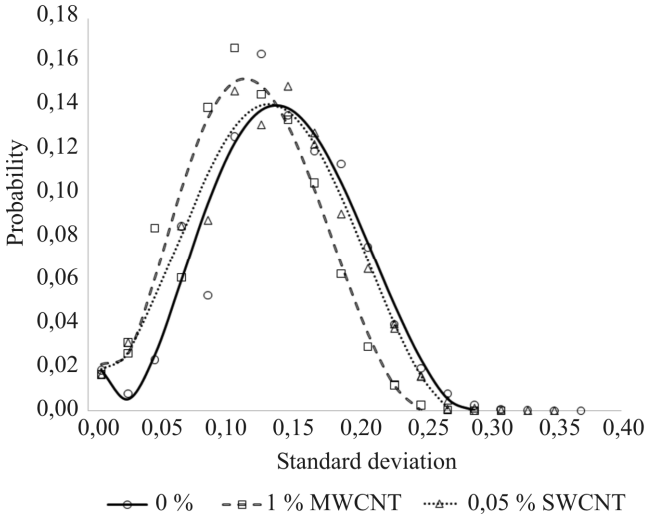

Fig. 4. Graph of the probability density function

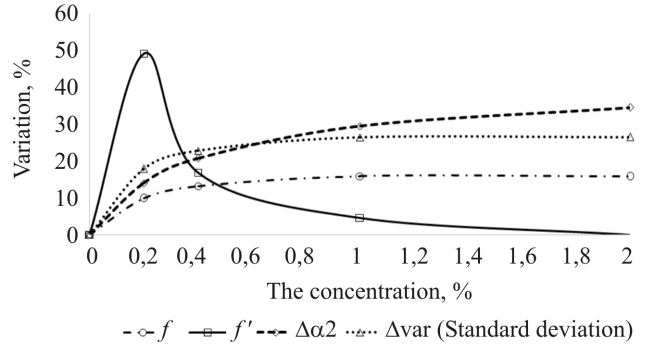

Fig. 5. Graph of the dependence of the variation in the indices of the standard deviation change sample on the concentration of multi-wall nanotubes

The warpage were obtained for each combination of the reinforcing fibers orientations on the basis of the data presented. The mathematical expectation of the standard deviation values of warpage is 0.1418 for the unmodified resin, 0.1372 for the samples based on the resin modified with single-walled nanotubes, 0.119 for the samples based on the resin modified with multi-walled nanotubes. It corresponds to decrease in standard deviation by 3.24 % and 15.95 % when modified with single-walled and multi-walled nanotubes, respectively. The sample variance also decreased by 12.6 % in the case of single-walled nanotubes, and by 26.6 % in the case of multi-walled ones. The size of each sample is equal to $\overline{A}_{14}^3 = 2744$, with a maximum disorientation angle of 2 degrees. The maximum disorientation angle was determined in terms of the dependence of the efficiency of modification of the composite material polymer matrix with carbon nanotubes, expressed by decrease in the mathematical expectation of the standard deviation compared to the same indicator for the composite material based on unmodified resin, on the maximum disorientation angle. The efficiency of modification has nonlinear dependence and decreases with increasing disorientation angle. For single-walled nanotubes, at the concentration of 0.05 %, the reduction in the modification efficiency was from 11 % to 5 % with increase in the disorientation angle from 0 to 2 degrees, and 37 % and 20 % for multi-walled nanotubes with similar increase in the disorientation angle.

Figure 4 shows the graphs of the probability density function for the standard deviation of the simulated surface of a composite plate based on unmodified and modified epoxy resins, taking into account the fibers disorientation.

Further, on the basis of the models described above we constructed the relations of the accuracy of the composite plate surface, expressed in terms of the standard deviation change, to the concentration of the modifier, taking into account the possible disorientation of the reinforcing fibers. When constructing the relations, we relied on the calculated thermoelastic characteristics of the modified epoxy resins and did not take into account the decrease in the efficiency of the modifier with the increase in the concentration in relation to the epoxy resin CTE. Despite this, the effectiveness of the modifier in improving the accuracy of the surface decreases with increasing its concentration.

Figure 5 shows the relations f of the standard deviation change of the composite plate to the concentration of the modifier, the derivative of f' with respect to the modifier concentration, the relation of the change in the variance of the standard deviation sample (ΔVar (Standard deviation)) to the modifier concentration and the relation of the change in the calculated transverse CTE of an elementary layer of the composite material (Δα2) to the modifier concentration. On the basis of data provided it can be concluded that it is inappropriate to use modifier concentrations above 1 % in order to reduce the warpage and the sample variance.

The samples were made of fabric based on fiber IMS 65 and unmodified or modified epoxy resin and have a reinforcement scheme [0/60/–60]. The samples have thickness 0.24 mm and the size of plate in the XY plane: 200×200 mm. The standard deviation of warpage was 0.1636 for the unmodified resin and 0.1329 for the resin modified with single-walled nanotubes, which corresponds to decrease in the standard deviation of warpage by 18.77 %.

Conclusions

We have measured the rheological properties of dispersion and thermomechanical properties of the obtained nanocomposites. The most effective modifiers and their concentrations were determined. For native nanotubes, the effective concentration is 0.05 %, which provides decrease in the CTE of the polymer matrix by 9.7 % with increase in viscosity to 0.83 Pa×s. Further increase in concentration is impossible due to the achieved high viscosity. For modified MWCNTs, concentration of 1 % is effective, providing decrease in CTE by 15.4 % and increase in viscosity up to 0.23 Pa×s. The thermomechanical properties of nanostructured laminated composite materials were investigated. It was found that carbon nanomodifiers are more effective as compensators for the thermal expansion of the polymer matrix in the fiber/epoxy laminated composites. The transverse CTE of unidirectional composite material decreased by 15.56 % in the cases of using native carbon nanotubes and by 35.8 % in the cases of using functionalized MWCNTs. Mathematical modeling of the warpage of plate, taking into account the possible disorientation of the fiber, showed decrease in standard deviation by 3.24 % and 15.95 % and decrease in sample variance by 12.6 % and 26.6 % when modified with single-walled and multi-walled nanotubes, respectively. On the basis of the obtained results, the dependences of the transverse CTE of an elementary layer of the composite material, the mathematical expectation of the standard deviation, and the variance of the standard deviation of the composite plate on the concentration of the modifier were constructed. According to the obtained data, it can be concluded that in order to reduce the mathematical expectation and the variance of the warping of the plate, there is an effective concentration, the increase of which is impractical, despite the further decrease in the transversal CTE. The results obtained confirm that the addition of carbon nanoparticles as a modifier to the polymer matrix can increase the accuracy and technological stability of the fiber composite quasi-isotropic reinforcement scheme.

Declaration of interests

The authors declare that they have no known competing financial interests or personal relationships that could have appeared to influence the work reported in this paper.

Appendix 1

The Mori-Tanaka's equation for the effective CTE of a filler-reinforced polymer matrix [55]:

$$\boldsymbol{\alpha} = \boldsymbol{\alpha}_{\mathbf{m}} + V_f \cdot \left\{ \mathbf{C}_{\mathbf{m}} + \left(\mathbf{C}_{\mathbf{f}} - \mathbf{C}_{\mathbf{m}} \right) \cdot \left[\left(1 - V_f \right) \cdot \mathbf{S} + V_f \cdot \mathbf{I} \right] \right\}^{-1} \cdot \cdot \mathbf{C}_{\mathbf{f}} \cdot \left(\boldsymbol{\alpha}_{\mathbf{f}} - \boldsymbol{\alpha}_{\mathbf{m}} \right).$$

Where $\boldsymbol{\alpha}_{\mathbf{m}}$ and $\boldsymbol{\alpha}_{\mathbf{f}}$ are the CTE of the resin and modifier, respectively, V_f is the volumetric content of the filler, $\mathbf{C}_{\mathbf{m}}$ is the stiffness matrix of the resin, $\mathbf{C}_{\mathbf{f}}$ is the stiffness matrix of the filler, $\mathbf{S}$ is the Eshelby tensor, $\mathbf{I}$ is the unit matrix.

Eshelby tensor S for the case of reinforcement with infinitely long elliptical cylinder in simplified form is [53]

$$\mathbf{S} = \begin{bmatrix} S_{1111} & S_{1122} & S_{1133} & 0 & 0 & 0 \\ S_{2211} & S_{2222} & S_{2233} & 0 & 0 & 0 \\ S_{3311} & S_{3322} & S_{3333} & 0 & 0 & 0 \\ 0 & 0 & 0 & S_{2323} & 0 & 0 \\ 0 & 0 & 0 & 0 & S_{1313} & 0 \\ 0 & 0 & 0 & 0 & 0 & S_{1212} \end{bmatrix}$$

$$S_{1111} = S_{1122} = S_{1133} = 0$$

$$S_{2222} = \frac{1}{2\left(1-\upsilon_m\right)}\left[\frac{b^2+2ab}{\left(a+b\right)^2} + \left(1-2\upsilon_m\right)\frac{b}{a+b}\right]$$

$$S_{3333} = \frac{1}{2\left(1-\upsilon_m\right)}\left[\frac{a^2+2ab}{\left(a+b\right)^2} + \left(1-2\upsilon_m\right)\frac{a}{a+b}\right]$$

$$S_{2233} = \frac{1}{2\left(1-\upsilon_m\right)}\left[\frac{b^2}{\left(a+b\right)^2} - \left(1-2\upsilon_m\right)\frac{b}{a+b}\right]$$

$$S_{3322} = \frac{\upsilon_m}{2\left(1-\upsilon_m\right)}\left[\frac{a^2}{\left(a+b\right)^2} - \left(1-2\upsilon_m\right)\frac{a}{a+b}\right]$$

$$S_{3311} = \frac{1}{2\left(1-\upsilon_m\right)} \cdot \frac{2\upsilon_m a}{a+b}$$

$$S_{2211} = \frac{1}{2\left(1-\upsilon_m\right)} \cdot \frac{2\upsilon_m b}{a+b}$$

$$S_{2323} = \frac{1}{2\left(1-\upsilon_m\right)} \cdot \left[\frac{a^2+b^2}{2\left(a+b\right)^2} + \frac{1-2\upsilon_m}{2}\right]$$

$$S_{1313} = \frac{a}{2\left(a+b\right)}$$

$$S_{1212} = \frac{b}{2\left(a+b\right)},$$

υ_m is the Poisson's ratio of the matrix, a and b are the main and auxiliary semi axes, respectively.

The effective CTE of a polymer matrix modified with three-dimensionally randomly distributed filler can be determined from the equation:

$$\alpha^c = \frac{1}{3} \cdot \alpha_{11} + \frac{2}{3} \cdot \alpha_{22}.$$

Where α_{11} and α_{22} are the longitudinal and transverse CTEs determined from the Mori-Tanaka's equation.

The Mori-Tanaka's equation for the effective Young's modulus of a polymer matrix reinforced with filler [55]:

$$\mathbf{C} = \left[\left(1-V_f\right)\cdot\mathbf{C_m} + V_f\cdot\mathbf{C_f}\cdot\mathbf{A}\right]\cdot\left[\left(1-V_f\right)\cdot\mathbf{I} + V_f\cdot\mathbf{A}\right]^{-1}$$

$$\mathbf{A} = \left[\mathbf{I} + \mathbf{S}\cdot\mathbf{C_m}^{-1}\cdot\left(\mathbf{C_f} - \mathbf{C_m}\right)\right]^{-1}.$$

Determination of the effective Young's modulus of resin modified with three-dimensionally randomly distributed filler [55]:

$$E^m = \frac{1}{5}\cdot E_{11} + \frac{4}{5}\cdot E_{22}.$$

Where E^m is the Young's modulus of the resin modified with three-dimensionally randomly distributed filler, E_{11} and E_{22} are the longitudinal and transverse Young's modulus, respectively, determined from the Mori-Tanaka's equation.

References

1. Shokrieh M.M., Daneshvar A., Akbari S., Chitsazzadeh M. The use of carbon nanofibers for thermal residual stress reduction in carbon fiber/epoxy laminated composites. *Carbon N Y,* 2013, no. 59, pp. 255-263. https://doi.org/10.1016/j.carbon.2013.03.016.

2. Ghasemi A.R., Mohammadi M.M., Mohandes M. The role of carbon nanofibers on thermo-mechanical properties of polymer matrix composites and their effect on reduction of residual stresses. *Compos Part B Eng,* 2015, no. 77, pp. 519-27. https://doi.org/10.1016/j.compositesb.2015.03.065.

3. Krause B., Pötschke P., Ilin E., Predtechenskiy M. Melt mixed SWCNT-polypropylene composites with very low electrical percolation. *Polymer,* 2016, no. 98, pp. 45-50. https://doi.org/10.1016/j.polymer.2016.06.004.

4. Clancy A.J., White E.R., Tay H.H., Yau H.C., Shaffer MS.P. Systematic comparison of conventional and reductive single-walled carbon nanotube purifications. *Carbon N Y*, 2016, no. 108, pp. 423-432. https://doi.org/10.1016/j.carbon.2016.07.034.

5. OCSiAl. TUBALL Technical Info https://tuball.com/en/about-tuball

6. Chung DDL. Carbon Fibers, Nanofibers, and Nanotubes. *Carbon Compos,* 2017, no. 1 (87). https://doi.org/10.1016/b978-0-12-804459-9.00001-4

7. Li F., Cheng H.M., Bai S., Su G., Dresselhaus M.S. Tensile strength of single-walled carbon nanotubes directly measured from their macroscopic ropes. *ApplPhysLett,* 2000, no. 77, pp. 3161-3163. https://doi.org/10.1063/1.1324984.

8. Demczyk B.G., Wang Y.M., Cumings J., Hetman M., Han W., Zettl A., et al. Direct mechanical measurement of the tensile strength and elastic modulus of multiwalled carbon nanotubes, *Mater SciEng A,* 2002, no. 334, pp. 173-178. https://doi.org/10.1016/S0921-5093 (01) 01807-X.

9. Spitalsky Z., Tasis D., Papagelis K., Galiotis C. Carbon nanotube-polymer composites: Chemistry, processing, mechanical and electrical properties. *ProgPolymSci*, 2010, no. 35, pp. 357-401. https://doi.org/10.1016/j.progpolymsci.2009.09.003.

10. Shirasu K., Nakamura A., Yamamoto G., Ogasawara T., Shimamura Y., Inoue Y., et al. Potential use of CNTs for production of zero thermal expansion coefficient composite materials: An experimental evaluation of axial thermal expansion coefficient of CNTs using a combination of thermal expansion and uniaxial tensile tests. *Compos Part A ApplSciManuf,* 2017, no. 95, pp. 152-160. https://doi.org/10.1016/j.compositesa.2016.12.027.

11. Ruoff R.S., Lorents D.C. Mechanical and thermal properties of carbon nanotubes. *Carbon* 1995, no. 33, pp. 925-930. https://doi.org/10.1016/0008-6223 (95) 00021-5.

12. Singh N.P., Gupta V.K., Singh A.P. Graphene and carbon nanotube reinforced epoxy nanocomposites: *A review. Polymer (Guildf),* 2019, no. 180. https://doi.org/10.1016/j.polymer.2019.121724.

13. Shokrieh M.M., Daneshvar A., Akbari S. *Reduction of thermal residual stresses of laminated polymer composites by addition of carbon nanotubes,* 2014, no. 53, pp. 209-216. https://doi.org/10.1016/j.matdes.2013.07.007.

14. Polymer nanocomposites. *MRS Bull,* 2007, no. 32, pp. 314-319. https://doi.org/10.1557/mrs2007.229.

15. Xie X.L., Mai Y.W., Zhou X.P. Dispersion and alignment of carbon nanotubes in polymer matrix: A review. *Mater SciEng R Reports,* 2005, no. 49, pp. 89-112. https://doi.org/10.1016/j.mser.2005.04.002.

16. Kim P., Shi L., Majumdar A., McEuen P.L. Thermal transport measurements of individual multiwalled nanotubes. *Phys Rev Lett,* 2001, no. 87. https://doi.org/10.1103/physrevlett.87.215502.

17. Fu S., Sun Z., Huang P., Li Y., Hu N. Some basic aspects of polymer nanocomposites: A critical review. *Nano Mater Sci*, 2019, no. 1, pp. 2-30. https://doi.org/10.1016/j.nanoms.2019.02.006.

18. Yu M.F., Lourie O., Dyer M.J., Moloni K, Kelly T.F., Ruoff R.S. Strength and breaking mechanism of multiwalled carbon nanotubes under tensile load. *Science* (80), 2000, no. 287, pp. 637-640. https://doi.org/10.1126/science.287.5453.637.

19. Breuer O., Sundararaj U. Big returns from small fibers: A review of polymer/carbon nanotube composites. *Polym Compos 2004*, no. 25, pp. 630-45. https://doi.org/10.1002/pc.20058.

20. Tibbetts G.G., Lake M.L., Strong K.L., Rice B.P. A review of the fabrication and properties of vapor-grown carbon nanofiber/polymer composites. *Compos SciTechnol*, 2007, no. 67, pp. 1709-18. https://doi.org/10.1016/j.compscitech.2006.06.015.

21. Eatemadi A., Daraee H., Karimkhanloo H., Kouhi M., Zarghami N., Akbarzadeh A, et al. Carbon nanotubes: Properties, synthesis, purification, and medical applications. *Nanoscale Res Lett 2014*, no. 9, pp. 1-13. https://doi.org/10.1186/1556-276X-9-393.

22. Annu A., Bhattacharya B., Singh P.K., Shukla P.K., Rhee H.W. Carbon nanotube using spray pyrolysis: Recent scenario. *J Alloys Compd,* 2017, no. 691, pp. 970-82. https://doi.org/10.1016/j.jallcom.2016.08.246.

23. Shirasu K., Yamamoto G., Tamaki I., Ogasawara T., Shimamura Y., Inoue Y., et al. Negative axial thermal expansion coefficient of carbon nanotubes: Experimental determination based on measurements of coefficient of thermal expansion for aligned carbon nanotube reinforced epoxy composites. *Carbon N Y*, 2015, no. 95, pp. 904-9. https://doi.org/10.1016/j.carbon.2015.09.026.

24. Kwon Y.K., Berber S., Tománek D. Thermal Contraction of Carbon Fullerenes and Nanotubes. *Phys Rev Lett*, 2004, no. 92, pp. 4. https://doi.org/10.1103/PhysRevLett.92.015901.

25. Ajayan P.M., Stephan O., Colliex C., Trauth D. Aligned carbon nanotube arrays formed by cutting a polymer resin-

nanotube composite. Science (80) 1994, no. 265, pp. 1212-4. https://doi.org/10.1126/science.265.5176.1212.

26. Garg A., Sinnott S.B. Effect of chemical functionalization on the mechanical properties of carbon nanotubes. *ChemPhysLett*, 1998, no. 295, pp. 273-8. https://doi.org/10.1016/S0009-2614 (98) 00969-5.

27. Shokrieh M.M., MasoudKamali S. Theoretical and experimental studies on residual stresses in laminated polymer composites. *J Compos Mater,* 2005, no. 39, pp. 2213-25. https://doi.org/10.1177/0021998305053511.

28. Shokrieh M.M., Akbari S., Daneshvar A. Reduction of residual stresses in polymer composites using nano-additives. *Residual Stress Compos Mater,* 2014, pp. 350-73. https://doi.org/10.1533/9780857098597.2.350.

29. Hahn H.T., Pagano N.J. Curing Stresses in Composite Laminates. *J Compos Mater* 1975, no. 9, pp. 91-106. https://doi.org/10.1177/002199837500900110.

30. Kurtz R.D., Pagano N.J. Analysis of the deformation of a symmetrically-loaded fiber embedded in a matrix material. *ComposEng,* 1991, no. 1, pp. 13-27. https://doi.org/10.1016/0961-9526 (91) 90022-K.

31. Huang Z.M. Strength formulae of unidirectional composites including thermal residual stresses. *Mater Lett* 2000, no. 43, pp. 36-42. https://doi.org/10.1016/S0167-577X (99) 00227-X.

32. Papanicolaou G.C., Michalopoulou M.V., Anifantis N.K. Thermal stresses in fibrous composites incorporating hybrid interphase regions. *Compos SciTechnol*, 2002, no. 62, pp. 1881-94. https://doi.org/10.1016/S0266-3538 (02) 00103-3.

33. Hashin Z, Walter Rosen B. The elastic moduli of fiber-reinforced materials. *J ApplMech Trans ASME* 1964, no. 31, pp. 223-32. https://doi.org/10.1115/1.3629590.

34. Steven Johnson W., Masters J., Kevin O'Brien T., Naik R. Simplified Micromechanical Equations for Thermal Residual Stress Analysis of Coated Fiber Composites. *J Compos Technol Res* 1992, no. 14, pp. 182. https://doi.org/10.1520/ctr10096j.

35. K. Jayaraman, K.L. Reifsnider. Residual stresses in a composite with continuously varying Young's modulus in the fiber/matrix interphase. *J Compos Mater*, 1992, vol. 26 (6), pp. 770-791.

36. Jayaraman K., Reifsnider K.L. Residual Stresses in a Composite with Continuously Varying Young's Modulus in the Fiber/Matrix Interphase. *J Compos Mater*, 1992, no. 26, pp. 770-91. https://doi.org/10.1177/002199839202600601.

37. Bianchi V., Goursat P., Ménessier E. Carbon-fiber-reinforced ymas glass-ceramic-matrix composites - IV. Thermal residual stresses and fiber/matrix interfaces. *Compos SciTechno*l 1998, no. 58, pp. 409-18. https://doi.org/10.1016/s0266-3538 (97) 00139-5.

38. Hsueh C.H., Becher P.F. Thermal Expansion Coefficients of Unidirectional Fiber-Reinforced Ceramics. *J Am Ceram Soc* 1988, vol. 71, pp. C438-41. https://doi.org/10.1111/j.1151-2916.1988.tb07521.x.

39. Epstein M. The Eshelby tensor and the theory of continuous distributions of inhomogeneities. *Mech Res Commun*, 2002, no. 29, pp. 501-6. https://doi.org/10.1016/S0093-6413 (02) 00303-8.

40. Shokrieh M.M., Safarabadi M. Effects of imperfect adhesion on thermal micro-residual stresses in polymer matrix composites. *Int J AdhesAdhes,* 2011, no. 31, pp. 490-7. https://doi.org/10.1016/j.ijadhadh.2011.04.002.

41. Abdalla M., Dean D., Theodore M., Fielding J., Nyairo E., Price G. Magnetically processed carbon nanotube/epoxy nanocomposites: Morphology, thermal, and mechanical properties. *Polymer (Guildf),* 2010, no. 51, pp. 1614-20. https://doi.org/10.1016/j.polymer.2009.05.059.

42. Green K.J., Dean D.R., Vaidya U.K., Nyairo E. Multiscale fiber reinforced composites based on a carbon nanofiber/epoxy nanophased polymer matrix: Synthesis, mechanical, and thermomechanical behavior. *Compos Part A ApplSciManuf*, 2009, no. 40, pp. 1470-5. https://doi.org/10.1016/j.compositesa.2009.05.010.

43. Hummers WS, Offeman RE. Preparation of Graphitic Oxide. *J Am ChemSoc,* 1958, no. 80 pp. 1339. https://doi.org/10.1021/ja01539a017.

44. Chen Y., Xu C., Hou Z., Zhou M., He B., Wang W., et al. 3D N, S-co-doped carbon nanotubes/graphene/MnS ternary hybrid derived from Hummers' method for highly efficient oxygen reduction reaction. *Mater Today Energy*, 2020, no. 16. https://doi.org/10.1016/j.mtener.2020.100402.

45. ООО "НаноТехЦентр», available at: http://www.nanotc.ru/producrions/87-cnm-taunit

46. Catalysis, available at: http://www.catalysis.ru/block/index.php?ID=3&SECTION_ID=1501

47. Ouarhim W., Hassani F.S., Qaiss A.K., Bouhfid R. Rheology of polymer nanocomposites. *RheolPolym Blends Nanocomposites Theory, Model Appl*, 2019, pp. 73-96. https://doi.org/10.1016/B978-0-12-816957-5.00005-7.

48. Nadiv R., Fernandes R.MF., Ochbaum G., Dai J., Buzaglo M., Varenik M., et al. Polymer nanocomposites: Insights on rheology, percolation and molecular mobility. *Polymer (Guildf),* 2018, no. 153, pp. 52-60. https://doi.org/10.1016/j.polymer.2018.07.079.

49. Bauhofer W., Kovacs J.Z. A review and analysis of electrical percolation in carbon nanotube polymer composites. *Compos SciTechnol,* 2009, no. 69, pp. 1486-98. https://doi.org/10.1016/j.compscitech.2008.06.018.

50. Sandler J.K.W, Kirk J.E., Kinloch I.A., Shaffer M.S.P, Windle A.H. Ultra-low electrical percolation threshold in carbon-nanotube-epoxy composites. *Polymer (Guildf)* 2003, no. 44, pp. 5893-9. https://doi.org/10.1016/S0032-3861 (03) 00539-1.

51. Pan J., Bian L. A physics investigation for influence of carbon nanotube agglomeration on thermal properties of composites. *Mater ChemPhys*, 2019, no. 236. https://doi.org/10.1016/j.matchemphys.2019.121777.

52. Mori T., Tanaka K. Average stress in matrix and average elastic energy of materials with misfitting inclusions. *ActaMetall*, 1973, no. 21, pp. 571-4. https://doi.org/10.1016/0001-6160 (73) 90064-3.

53. Raju B., Hiremath S.R., Roy Mahapatra D. A review of micromechanics based models for effective elastic properties of reinforced polymer matrix composites. *Compos Struct*, 2018, no. 204, pp. 607-19. https://doi.org/10.1016/j.compstruct.2018.07.125.

54. Kazakov I.A., Krasnovskii A.N., Kishuk P.S. The influence of randomly oriented CNTs on the elastic properties of unidirectionally aligned composites. *Mech Mater*, 2019, no. 134, pp. 54-60. https://doi.org/10.1016/j.mechmat.2019.04.002.

55. Dong C. Mechanical and thermo-mechanical properties of carbon nanotube reinforced composites. *Int J Smart Nano Mater,* 2014, no. 5, pp. 44-58. https://doi.org/10.1080/19475411.2014.896427.

56. Chang T., Gao H. Size-dependent elastic properties of a single-walled carbon nanotube via a molecular mechanics model. *J MechPhys Solids*, 2003, no. 51, pp. 1059-74. https://doi.org/10.1016/S0022-5096 (03) 00006-1.

57. Stobinski L., Lesiak B., Kövér L., Tóth J., Biniak S., Trykowski G., etal. Multiwall carbon nanotubes purification and oxidation by nitric acid studied by the FTIR and electron spectroscopy methods. *J Alloys Compd,* 2010, no. 50, pp. 77-84. https://doi.org/10.1016/j.jallcom.2010.04.032.

58. Takao Y., Taya M. Thermal expansion coefficients and thermal stresses in an aligned short fiber composite with application to a short carbon fiber/aluminum. *J ApplMech Trans ASME,* 1985, no. 52, pp. 806-10. https://doi.org/10.1115/1.3169150.

59. Rosen B.W., Hashin Z. Effective thermal expansion coefficients and specific heats of composite materials. *Int J EngSci,* 1970, no. 8, pp. 157-73. https://doi.org/10.1016/0020-7225(70)90066-2.

60. Hyer M.W. Calculations of the Room-Temperature Shapes of Unsymmetric Laminates. *J Compos Mater,* 1981, no. 15, pp. 296-310. https://doi.org/10.1177/002199838101500401.

61. Dano M.L., Hyer M.W. Thermally-induced deformation behavior of unsymmetric laminates. *Int J Solids Struct,* 1998, no. 35, pp. 2101-20. https://doi.org/10.1016/S0020-7683(97)00167-4.

62. Betts D.N., Salo A.I.T, Bowen C.R., Kim H.A. Characterisation and modelling of the cured shapes of arbitrary layup bistable composite laminates. *Compos Struct,* 2010, no. 92, pp. 1694-700. https://doi.org/10.1016/j.compstruct.2009.12.005.

63. Pradere C., Sauder C. Transverse and longitudinal coefficient of thermal expansion of carbon fibers at high temperatures (300-2500 K). *Carbon N Y*, 2008, no. 46, pp. 1874-84. https://doi.org/10.1016/j.carbon.2008.07.035.

64. Duan S., Liu F., Pettersson T., Creighton C., Asp L.E. Determination of transverse and shear moduli of single carbon fibres. *Carbon N Y*, 2020, no. 158, pp. 772-82. https://doi.org/10.1016/j.carbon.2019.11.054.

65. Mehanicheskie svojstva modificirovannyh odnostennymi uglerodnymi nanotrubkami jepoksidnyh svjazujushhih dlja armirovannyh kompozicionnyh materialov. Vestnik Voronezhskogo Gosudarstvennogo Tehnicheskogo Universiteta, 2016, pp. 12.

66. Guo F., Yan Y., Hong Y., Li X., Ye J. Theoretical prediction for thermal expansion coefficients of unidirectional fiber-reinforced composites with variable elliptical cross-sections. *Polym Compos,* 2019, no. 40, pp. 187-201. https://doi.org/10.1002/pc.24627.

67. Daniel I.M, Ishai O. Engineering Mechanics of Composite Material. Second ed. New York: Oxford University Press, 2006.

68. Asprotec, available at: http://www.asprotec.ru/pub/IMS65_E23.pdf

69. Herráez M., Mora D., Naya F., Lopes C.S., González C., Llorca J. Transverse cracking of cross-ply laminates: A computational micromechanics perspective. *Compos SciTechnol*, 2015, no. 110, pp. 196-204. https://doi.org/10.1016/j.compscitech.2015.02.008.

70. Toraycma, available at: https://www.toraycma.com/file_viewer.php?id=5121

71. Maurin R., Davies P., Baral N., Baley C. Transverse properties of carbon fibres by nano-indentation and micro-mechanics. *Appl Compos Mater,* 2008, no. 15, pp. 61-73. https://doi.org/10.1007/s10443-008-9057-3.

72. Ran Z., Yan Y., Li J., Qi Z., Yang L. Determination of thermal expansion coefficients for unidirectional fiber-reinforced composites. *Chinese J Aeronaut*, 2014, no. 27. pp. 1180-7. https://doi.org/10.1016/j.cja.2014.03.010.

73. Arao Y., Koyanagi J., Utsunomiya S., Kawada H. Effect of ply angle misalignment on out-of-plane deformation of symmetrical cross-ply CFRP laminates: Accuracy of the ply angle alignment. *Compos Struct*, 2011, no. 93, pp. 1225-30. https://doi.org/10.1016/j.compstruct.2010.10.019.

74. Steeves J., Pellegrino S. Post-cure shape errors of ultra-thin symmetric CFRP laminates: Effect of ply-level imperfections. *Compos Struct,* 2017, no. 164, pp. 237-47. https://doi.org/10.1016/j.compstruct.2016.12.075.

Благодарности. Работа выполнена коллективом научной лаборатории «Интеллектуальные материалы и конструкции» в рамках государственного задания Министерства науки и высшего образования Российской Федерации на реализацию проекта «Разработка многофункциональных интеллектуальных материалов и конструкций на основе модифицированных полимерных композиционных материалов, способных функционировать в экстремальных условиях» (проект № ФЭФЭ-2020-0015). Изображения углеродных нанотрубок были получены с помощью просвечивающего электронного микроскопа Hitachi HT7700 в Красноярском краевом центре исследовательского оборудования Федерального исследовательского центра «Красноярский научный центр СО РАН».

Конфликт интересов. Авторы заявляют об отсутствии конфликта интересов.

Acknowledgments. This work was carried out by the team of the scientific laboratory “Smart Materials and Structures” within the state assignment of the Ministry of Science and Higher Education of the Russian Federation for the implementation of the project “Development of multifunctional smart materials and structures based on modified polymer composite materials capable to function in extreme conditions” (Project No. FEFE-2020-0015). Images of carbon nanotubes were obtained using a Hitachi HT7700 transmission electron microscope in the Krasnoyarsk Regional Center of Research Equipment of Federal Research Center “Krasnoyarsk Science Center SB RAS”.

Conflict of interest. The authors declare no conflict of interest.